Journal of Alloys and Compounds 508 (2010) 106–109

Contents lists available at ScienceDirect

Journal of Alloys and Compounds

journal homepage: www.elsevier.com/locate/jallcom

Low-temperature fabrication and properties of the highly oriented $Bi_{3.15}Nd_{0.85}Ti_3O_{12}$ thin films deposited on different substrates

Z.Y. Lu, C.H. Yang, G.D. Hu*, J.C. Wang, X. Wang

School of Materials Science and Engineering, University of Jinan, Jiwei Road 106, Jinan 250022, Shandong, PR China

ARTICLE INFO

Article history:
Received 25 January 2010
Received in revised form 12 May 2010
Accepted 21 May 2010
Available online 1 June 2010

PACS:
77.84.–s
81.20.Ka
85.50.Gk

Keywords:
Ferroelectrics
Chemical synthesis
Thin film

ABSTRACT

$Bi_{3.15}Nd_{0.85}Ti_3O_{12}$ (BNdT) films have been prepared on $Pt/TiO_2/SiO_2/Si$ and $(Ba_{0.5}Sr_{0.5})(Ti,Mn)O_3$ (BSTMn)/n-Si substrates using a metal organic decomposition method. X-ray patterns show the BNdT films with highly *a*-axis and (1 1 7) orientation were fabricated by the sequential layer annealing method, which is further confirmed by the shapes of grains in the AFM images. The electrical measurements were conducted on metal–ferroelectric–metal (MFM) and metal–ferroelectric–insulator–semiconductor (MFIS) capacitors. The BNdT film in MFM capacitor exhibits a well-saturated hysteresis loop at an applied voltage of ±10 V, with a remanent polarization of 14.5 μC/cm^2 and a coercive field of 81.5 kV/cm. The BSTMn buffer layer is calculated to be about 30 nm by comparing the capacitance-voltage curves with polarization-electric field loops. The ferroelectric and charge injection effects for MFIS are analyzed in detail at various applied voltages. The largest memory window of MFIS is as large as 4.5 V.

1. Introduction

Ferroelectric materials in form of thin films have been extensively investigated for application to ferroelectric random access memories (FRAMs) because nondestructive readout is possible [1,2]. There are two types of FRAMs. One is the commercially available 1T1C type, where the data are memorized in a metal–ferroelectric–metal (MFM) capacitor [3]. The other is the 1T or transistor type. For this type, it is necessary to deposit ferroelectric film directly on semiconductor substrate to form a metal–ferroelectric–semiconductor (MFS) structure [4]. However, the interdiffusion and reaction of constituent elements between the ferroelectric film and Si substrate during the crystallization annealing usually occur. Many researches have demonstrated that the metal–ferroelectric–insulator–semiconductor (MFIS) can prevent the interface effect by inserting a high-quality buffer layer [5,6]. $(Ba_{0.5}Sr_{0.5})TiO_3$ film has been considered to be an effective diffusion barrier between the ferroelectric film and Si substrate [7,8]. Furthermore, Mn-doped (Ba,Sr)TiO_3 films have lower leakage current due to the acceptor behavior of Mn [9,10].

Lanthanides (La, Sm, Nd, and Pr)-doped $Bi_4Ti_3O_{12}$ (BLnT) thin films have attracted a lot of attention for applications in FRAMs [11,12]. The remanent polarization is enhanced due to that the structural distortion within the perovsike block takes place by doping with lanthanides. The spontaneous polarizations of $Bi_4Ti_3O_{12}$ are different along *a* and *c* axes due to its anisotropic pseudo-orthorhombic structure [13]. Several groups found that the major polarization vector of BLnT is close to the *a* axis [14–16]. In the previous work, we have prepared variously oriented $Bi_{3.15}Nd_{0.85}Ti_3O_{12}$ (BNdT) films, and confirmed each remanent polarization (Pr) value of the purely (1 0 0)-, (1 1 7)-, and (0 0 1)-oriented BNdT films [17]. We have also enhanced ferro- and piezo-electric properties of $Bi_{3.7}Nd_{0.3}Ti_3O_{12}$ film at 650 °C [18]. Such a low annealed temperature makes it possible to keep a satisfied compatibility and integration in the silicon technology.

In this paper, the BNdT films were synthesized by metal organic decomposition. At the annealed temperature of 650 °C, the highly *a*-axis and (1 1 7) oriented BNdT films were fabricated by the sequential layer annealing method. The $Pt/TiO_2/SiO_2/Si$ and $(Ba_{0.5}Sr_{0.5})(Ti,Mn)O_3$ (BSTMn)/Si were selected as substrates for the fabrication of MFM and MFIS devices. The properties of BNdT films on two different substrates are discussed.

2. Experimental procedure

A thin BSTMn layer was first formed on Si substrate. The detailed formation procedure of BSTMn film was reported elsewhere [19]. Similar to our previous work [17,18], the precursor solution of BNdT was prepared by a metal organic decomposition process, and then deposited on both $Pt/TiO_2/SiO_2/Si$ and BSTMn/Si using a sequential layer annealing method at 650 °C. We select the sequential layer anneal-

* Corresponding author. Tel.: +86 531 88374857; fax: +86 531 87974453.
E-mail address: gdhu@ujn.edu.cn (G.D. Hu).

0925-8388/$ – see front matter © 2010 Elsevier B.V. All rights reserved.
doi:10.1016/j.jallcom.2010.05.096

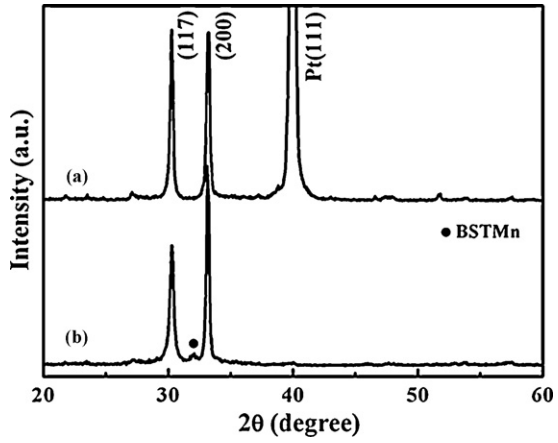

Fig. 1. The X-ray diffraction patterns of the highly *a*-axis and (1 1 7) oriented BNdT film annealed at 650 °C on (a) $Pt/TiO_2/SiO_2/Si$ and (b) BSTMn/Si substrates.

ing possess because that each crystallized layer can be used as a seeding layer for growing the next one [20], and the thermal stresses and evaporation of elements can be reduced [21]. The thickness of BNdT film was estimated to be about 300 nm by a step (step obtained by chemical etching) profilometer made by the Ambios Technology Company of USA.

The crystallization of BNdT film was studied by X-ray diffraction using a Rigaku D/MAX-γA X-ray diffractometer. The surface microstructures have been analyzed by a digital instrument multi-mode atomic force microscope (AFM). For measurements of electrical properties, Au dots were used as upper electrodes, and Au bottom electrode was used on the back of silicon substrate to form MFM and MFIS configurations. The ferroelectric property was conducted using a standard ferroelectric tester (Precision Pro. Radiant Tech., Albuquerque, NM). The capacitance–voltage curves were measured using an LF Impedance Analyzer (HP 4294A).

3. Results and discussion

Fig. 1 shows the XRD patterns of BNdT films on $Pt/TiO_2/SiO_2/Si$ and BSTMn/Si substrates. The BNdT films exhibit two strong peaks of (1 0 0) and (1 1 7) on both substrates. Similar to $Bi_{3.7}Nd_{0.3}Ti_3O_{12}$ film [18], the relative intensities of (1 0 0) and (1 1 7) peaks for BNdT film annealed at 650 °C are high due to the grain growth and competitive growth. Because the nucleation activation energy for BNdT decreases caused by the BSTMn buffer layer, the relative intensity of (2 0 0) peak [$I_{(200)}/I_{(117)}$] for BNdT on BSTMn is higher than on Pt. The bi-layered perovskite film on Pt usually needs higher annealing temperature to grow (1 0 0)-oriented grains [22]. The little peak marked by filled circle is corresponding to the (1 1 0) peak of BSTMn film.

The surface morphologies of BNdT films on two different substrates were detected using AFM in tapping mode. As can be seen from Fig. 2, there are two shapes of grains, namely, equiaxed and rodlike ones, which have been demonstrated to be (1 0 0)- and (1 1 7)-oriented in our earlier work [17]. The proportion of the rodlike grains in Fig. 2(a) is higher than that in Fig. 2(b), which is consistent with the XRD results. The root mean square surface roughness of BNdT film on Pt (5.85 nm) is slightly higher than on BSTMn (5.55 nm).

The remanent polarization (Pr) and coercive field (E_c) of Au/BNdT/Pt capacitor as a function of applied electric field are shown in Fig. 3. The corresponding ferroelectric hysteresis loops measured at various applied voltages ranging from ±2 to ±10 V are inserted in Fig. 3. This ferroelectric property points that the polarization process could be easily accomplished leading to a very regularly shaped hysteresis loop at ±10 V. The measured Pr and E_c of BNdT are 14.5 μC/cm² and 81.5 kV/cm, respectively, at an electric field of 333 kV/cm. This Pr is much higher than that of the $(Bi, La)_4Ti_3O_{12}$ annealed at the same temperature of 650 °C [23,24]. The polarization enhancement of our BNdT film may be attributed to

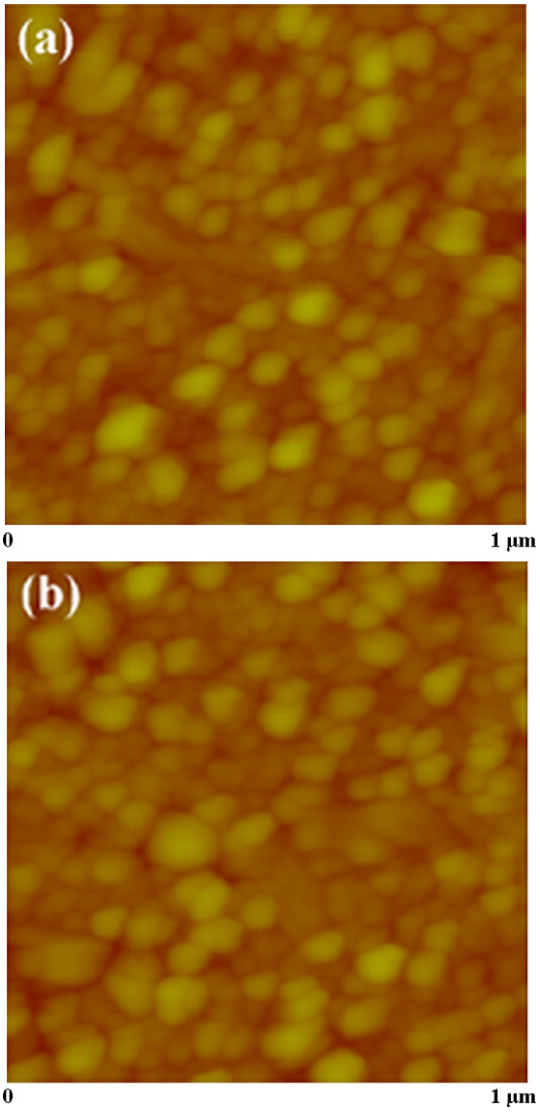

Fig. 2. AFM images of the highly *a*-axis and (1 1 7) oriented BNdT films annealed at 650 °C on (a) $Pt/TiO_2/SiO_2/Si$ and (b) BSTMn/Si substrates.

the following two reasons. (i) To compare the eightfold coordination ionic radii: Bi, 0.117 nm; La, 0.116 nm; Nd, 0.111 nm; Nd has a larger size difference from Bi. It can be deduced from these data that Nd doping will lead to larger distortion than La doping and should,

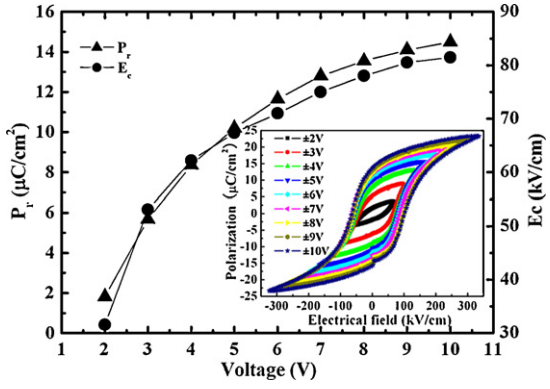

Fig. 3. Variations of Pr and E_c values of the Au/BNdT/Pt capacitor are plotted as a function of the applied voltage. The inset shows P–E hysteresis loops at various applied voltages.

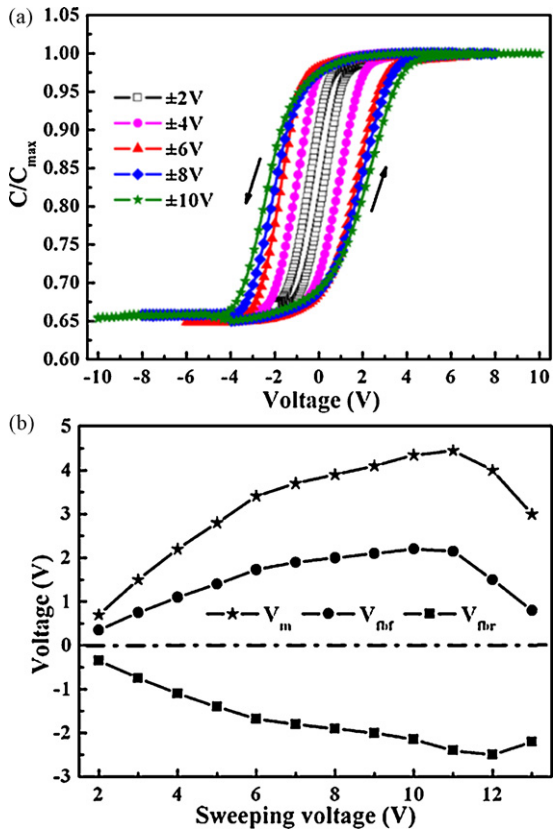

Fig. 4. (a) C–V properties of the Au/BNdT/BSTMn/Si MFIS structures measured at 1 MHz for voltages smaller than ±10 V. (b) The flatband voltage shifts (V_{fbf}, V_{fbr}) and memory window (V_m) vs sweeping voltage.

in principle, result in a larger Pr. (ii) It is known that the remnant polarization of BTO-based film is affected by the crystalline orientations. For BLnT films, $Pr_{(100)} > Pr_{(117)} > Pr_{(001)}$. A highly (1 0 0) and (1 1 7) oriented BNdT film was observed in the XRD pattern of BNdT/Pt/TiO_2/SiO_2/Si, as shown in Fig. 1. Therefore, a larger Pr of our sample is observed compared with (1 1 7)- and random-oriented BLnT films [24,25].

The C–V properties of Au/BNdT/BSTMn/Si were measured at a frequency of 1 MHz with a small AC signal of 300 mV amplitude under various voltages. We selected BSTMn as a buffer layer due to that the BSTMn film has a high dielectric constant of 30 and low leakage current density of less than 10^{-7} A/cm^2 when the applied voltage is not higher than 10 V (not shown here). The C–V curves of BNdT/BSTMn for sweeping voltages higher than ±10 V are not shown in Fig. 4(a) for clarity. The C–V results exhibit anticlockwise hysteresis loops on BSTMn/n-type Si substrate. The width of the memory window (V_m) is defined as the difference of the flatband voltage (V_{fb}) shift during the voltage sweeping. V_{fbf} and V_{fbr} are defined as the V_{fb} from the negative to positive bias and the V_{fb} from the positive to negative bias.

The memory window of C–V curve can be expressed by the following equation [26]: $V_m = (E_c^+ - E_c^-)d_f - V_i$, where V_m is the width of memory window; E_c^+ and E_c^- are the positive and negative coercive electric fields of the ferroelectric film, respectively; d_f is the thickness of the ferroelectric films; and V_i is the flatband voltage shift due to the charge injection. As we can see from Fig. 4(a), the C–V curves increases symmetrically when the sweeping voltage ranging from ±2 to ±10 V. This phenomenon is attributable to the increase of ferroelectric polarization of BNdT and the negligible charge injection [27]. Therefore, the charge trapping and charge injection effect are negligible (i.e., $V_i \sim 0$)[26]. Compared the C–V curves with the P–E loops in Fig. 3, we notice the memory window at a certain voltage is close to the $d_f(E_c^+ - E_c^-)$ at three-fifths of the certain voltage. For example, the V_m is 4.35 V at ±10 V. The coercive field ($E_c^+ - E_c^-$) of MFM capacitor under the applied voltage of ±6 V is 143 kV/cm. The memory window of MFIS at ±10 V is nearly equal to $d_f(E_c^+ - E_c^-)$ of MFM at ±6 V. Therefore, we infer that the ratio of voltage drop across BNdT and BSTMn is 3:2. The voltage drop across the ferroelectric layer (V_f) and the buffer layer (V_b) can be expressed as $V_f/V_b = d_f\varepsilon_b/d_b\varepsilon_f$ [28], where d_f, d_b, ε_f, and ε_b are the film thicknesses and the relatively dielectric constants of ferroelectric and buffer layers, respectively. We have measured the ε_f of the BNdT is about 220 in MFM structure. Therefore, the thickness of BSTMn is about 30 nm by calculating.

The Variations of V_{fbf}, V_{fbr} and V_m for BNdT with the sweeping voltage are shown in Fig. 4(b) for understanding the working mechanisms. When the voltage is lower than ±10 V, the V_{fbf} increases linearly and V_{fbr} decreases linearly, and the magnitude of V_{fbf} is nearly equal to that of V_{fbr}. These results suggest that the increase in memory window under ±10 V is only caused by ferroelectric polarization. As the voltage increases up to ±11 V, the V_{fbf} remains essentially constant and V_{fbr} decrease rapidly. Therefore, the degree of the positive shift for V_{fbf} is smaller than that of the negative shift for V_{fbr}. This can be attributed to the effect of trapped positive charges which result in negative shifts of both V_{fbf} and V_{fbr} [8,29]. When a higher negative bias of −11 V is initially applied on the top electrode, a small quantity of holes will be trapped in the BNdT/BSTMn, which in turn induces negative charges in the Si surface. When the voltage is swept from negative to positive direction, the V_{fbf} occurs at smaller voltage than in the case of no charge injection. Thus, the V_{fbf} will stop increasing. Similarly, the V_{fbr} will decrease rapidly. With the further increase of the sweeping voltage, the charge injection becomes evident and neutralizes the polarization charges of BNdT, resulting in the decrease in V_m for the applied voltage from ±12 V. It is noting that the largest memory window is 4.5 V, which is larger than that of other $Bi_4Ti_3O_{12}$-based MFIS structures, such as $Bi_{3.25}La_{0.75}Ti_3O_{12}$/$LaAlO_3$ [30] and $Bi_{3.15}La_{0.85}Ti_3O_{12}$/$Al_2O_3$ [31] $Bi_{3.4}Gd_{0.6}Ti_3O_{12}$/Si [32]. We attribute the larger V_m for BNdT/BSTMn to three major reasons: (i) the BSTMn can prevent the charge injection from the Si substrate effectively. (ii) The highly *a*-axis and (1 1 7) orientation growth mode for BNdT. (iii) The voltage drop across BNdT and BSTMn is reasonable due to the high dielectric constant and thin thickness of BSTMn. (iv) The low-temperature annealing process.

4. Conclusions

In conclusion, the BNdT thin films with highly (1 0 0) and (1 1 7) orientation are obtained annealed at the low-temperature of 650 °C layer by layer. The P–E hysteresis loops could be easily saturated at 333 kV/cm with a remanent polarization of 14.5 μC/cm^2 and a coercive field of 81.5 kV/cm. The thickness of BSTMn buffer layer is about 30 nm by calculating. The MFIS structure exhibits anticlockwise C–V curves due to the ferroelectric polarization of BNdT without charge injection within ±2∼± 10 V and the maximal memory window of MFIS is 4.5 V at ±11 V. These above results show that the BNdT films have potential for FRAMs

Acknowledgements

This work was supported by the Science and Technology Plan of Shandong provincial education department of China (no. J09LD19), the Outstanding Young Scientists Foundation Grant of Shandong Province (no. BS2009CL001), the Key Project of Chinese Ministry of Education (No.210121) and the National Natural Science Foundation of China (nos. 50972049 and 51002064).

References

[1] H. Irie, H. Saito, S. Ohkoshi, K. Hashimoto, Adv. Mater. 17 (2005) 491–494.
[2] J.F. Scott, C.A. Paz de Araujo, Science 246 (1989) 1400–1405.
[3] M.A. Khan, T.P. Comyn, A.J. Bell, Appl. Phys. Lett. 91 (2007) 032901–32903.
[4] C.H. Yang, H.T. Wu, D.M. Yang, Mater. Lett. 61 (2007) 4166–4168.
[5] C.H. Yang, G.D. Hu, Z. Wen, H.L. Yang, Appl. Phys. Lett. 93 (2008) 172906–172913.
[6] C.M. Lin, W.C. Shih, I.Y. Chang, P.C. Juan, J.Y. Lee, Appl. Phys. Lett. 94 (2009) 142905–142913.
[7] C.H. Liu, J.M. Wu, L.J. Wu, Appl. Phys. Lett. 88 (2006) 122901–122903.
[8] C.S. Yeh, J.M. Wu, Appl. Phys. Lett. 93 (2008) 154101–154103.
[9] K.T. Kang, I.I.-D. Kim, M.H. Lim, H.G. Kim, J.M. Hong, Thin Solid Films 516 (2008) 1218–1222.
[10] M. Jain, S.B. Majumder, R.S. Katiyar, Appl. Phys. Lett. 82 (2003) 1911–1913.
[11] H.N. Lee, D. Hesse, N. Zakharov, U. Gösele, Science 296 (2002) 2006–2009.
[12] C.H. Yang, S.D. Wang, D.M. Yang, J. Alloys Compd. 467 (2009) 434–437.
[13] A.D. Rae, J.G. Thompson, R.L. Withers, A.C. Willis, Acta Crystallogr., Sect. B: Struct. Sci. 46 (1990) 474–487.
[14] C.J. Lu, X.L. Liu, X.Q. Chen, C.J. Nie, G.L. Rhun, S. Senz, D. Hesse, Appl. Phys. Lett. 89 (2006) 062905–62913.
[15] G.D. Hu, S.H. Fan, X. Cheng, J. Appl. Phys. 101 (2007) 054111–54116.
[16] Z.X. Cheng, C.E. Kannan, K. Ozawa, H. Kimura, X.L. Wang, Appl. Phys. Lett. 89 (2006) 032901–32903.
[17] G.D. Hu, J. Appl. Phys. 100 (2006) 096109–96113.
[18] L.L. Jiao, A.M. Liu, G.D. Liu, S.G. Cui, Z.J. Jin, Q. Wang, W.B. Wu, C.H. Yang, J. Am. Ceram. Soc. 92 (2009) 1556–1559.
[19] M. Jain, S.B. Majumder, A. Martinez, R.S. Katiyar, F.W. Van Keuls, F.A. Miranda, Integr. Ferroelectr. 42 (2002) 343–355.
[20] T. Yu, K.W. Kwok, H.L.W. Chan, Thin Solid Films 515 (2007) 3563–3566.
[21] Y.C. Hsu, C.C. Wu, C.C. Lee, G.Z. Cao, I.Y. Shen, Sens. Actuators, A 116 (2004) 369–377.
[22] J. Yan, G.D. Hu, Z.M. Liu, S.H. Fan, Y. Zhou, C.H. Yang, W.B. Wu, J. Appl. Phys. 103 (2008) 056109–56113.
[23] B.H. Park, B.S. Kang, S.D. Bu, T.W. Noh, J. Lee, W. Jo, Nature (Lond.) 401 (1999) 682–684.
[24] K.T. Kim, C.I. Kim, Vacuum 74 (2004) 665–670.
[25] B.T. Liu, W.T. Zhang, Y. Wang, H.L. Sun, F. Li, Z. Yan, J. Du, Q.X. Zhao, Mater. Lett. 61 (2007) 1933–1936.
[26] S.K. Lee, Y.T. Kim, S. Kim, C.E. Lee, J. Appl. Phys. 91 (2002) 9303–9307.
[27] H.Y. Chen, J.M. Wu, H.E. Huang, H.Y. Bor, Appl. Phys. Lett. 90 (2007) 112907–112913.
[28] C.H. Chang, T.P. Juan, J.Y. Lee, Appl. Phys. Lett. 88 (2006) 072917–72923.
[29] T. Choi, Y.S. Kim, C.W. Yang, J. Lee, Appl. Phys. Lett. 79 (2001) 1516–1518.
[30] Y.J. Wang, A.D. Li, D. Wu, Q.Y. Shao, H.Q. Ling, X.B. Lu, Z.G. Liu, N.B. Ming, J. Phys. D: Appl. Phys. 37 (2004) 823–835.
[31] S.M. Jung, S.I. Yoo, Y.H. Kim, Y.T. Kim, S.K. Hong, J. Kor. Phys. Soc. 49 (2006) S552–S556.
[32] S.S. Kim, J.C. Bae, W.J. Kim, J. Cryst. Growth 274 (2005) 394–401.